AFRL-AFOSR-UK-TR-2013-0033

Unsteady Shock Waves Vortex Shedding Entanglement in a Transonic Turbine Cascade

Guillermo Paniagua

Institut Von Karman DE
Dynamique Des Fluides VZW
Waterloosesteenweg 72
Sint-Genesius-Rode, Belgium 1640

EOARD Grant 12-2119

Report Date: July 2013

Final Report from 1 July 2012 to 31 December 2012

Air Force Research Laboratory
Air Force Office of Scientific Research
European Office of Aerospace Research and Development
Unit 4515 Box 14, APO AE 09421

REPORT DOCUMENTATION PAGE

Form Approved OMB No. 0704-0188

1. REPORT DATE *(DD-MM-YYYY)*	2. REPORT TYPE	3. DATES COVERED *(From – To)*
30 July 2013	Final Report	1 July 2012 – 31 December 2012

4. TITLE AND SUBTITLE

Unsteady Shock Waves Vortex Shedding Entanglement in a Transonic Turbine Cascade

5a. CONTRACT NUMBER

FA8655-12-1-2119

5b. GRANT NUMBER

Grant 12-2119

5c. PROGRAM ELEMENT NUMBER

61102F

6. AUTHOR(S)

Guillermo Paniagua

5d. PROJECT NUMBER

5d. TASK NUMBER

5e. WORK UNIT NUMBER

7. PERFORMING ORGANIZATION NAME(S) AND ADDRESS(ES)

Institut Von Karman DE
Dynamique Des Fluides VZW
Waterloosesteenweg 72
Sint-Genesius-Rode, Belgium 1640

8. PERFORMING ORGANIZATION REPORT NUMBER

N/A

9. SPONSORING/MONITORING AGENCY NAME(S) AND ADDRESS(ES)

EOARD
Unit 4515 BOX 14
APO AE 09421

10. SPONSOR/MONITOR'S ACRONYM(S)

AFRL/AFOSR/IOE (EOARD)

11. SPONSOR/MONITOR'S REPORT NUMBER(S)

AFRL-AFOSR-UK-TR-2013-0033

12. DISTRIBUTION/AVAILABILITY STATEMENT

Distribution A: Approved for public release; distribution is unlimited.

13. SUPPLEMENTARY NOTES

14. ABSTRACT

This report describes the design and numerical analysis of a turbine cascade suitable to research the vortex shedding and shock waves coupling. This follows the very successful research model that was used to drive a 60% increase in lift beyond the state-of-the-art for Low Pressure Turbines (LPTs). The selected turbine flow passage enhanced the vortex shedding intensity by using a relatively large trailing edge diameter. This geometry is both government-owned and generic. So, the geometry and all experimental data produced in the study will be distributable throughout the research community, and this can further increase knowledge about the flowfield and additional means to control. A potential solution that is being explored is the use of pulsed cooling ejection to control both the vortex shedding and trailing edge shock patterns. The present research may guide aerodynamic designers to novel concepts to modulate shock waves.

The current research is high relevance for the design of compact and light future fluid machinery. While the results of such an investigation have bearing on transonic turbines and compressors in particular, the physics that dominate the flow are fundamental and could have applicability to any flow that is dominated by both shocks and vertical disturbances.

15. SUBJECT TERMS

EOARD, unsteady shock waves, turbine cascade,vortex shedding, shock wave interaction

16. SECURITY CLASSIFICATION OF:			17. LIMITATION OF ABSTRACT	18, NUMBER OF PAGES	19a. NAME OF RESPONSIBLE PERSON
a. REPORT	b. ABSTRACT	c. THIS PAGE			Gregg Abate
UNCLAS	UNCLAS	UNCLAS	SAR	18	19b. TELEPHONE NUMBER *(Include area code)* +44 (0)1895 616021

Contract FA8655-12-1-2119

Unsteady Shock Waves Vortex Shedding Entanglement in a Transonic Turbine Cascade

Guillermo Paniagua

von Karman Institute for Fluid Dynamics

Table of contents

1. Introduction

In transonic turbomachinery airfoils, both shock waves and wakes appear at the trailing edge, giving rise stator-rotor interactions that abate the turbine performance and durability. There is good insight into the physics of the shocks and vortices formation from the time-averaged point of view. In a turbomachine operating at high subsonic Mach number flow (0.96) Clark and Grover [1] found that the unsteady pressures that give rise to High Cycle Fatigue (HCF) in the blade row were dominated not by the typical frequencies associated with rotor/stator interaction but by inherent unsteadiness in the flow due to shock motion. The identified unsteadiness was broad-banded, suggesting that the shedding actually occurred at a frequency between 168E and 180E with an attendant picket-fence effect on the spectral analysis [2]. The hypothesis was that the unsteady blockage caused by the vortex shedding produces enough of an instantaneous variation in the throat area to cause unsteady shock motion with a frequency consistent with that of the von Karman vortices. Hence, high levels of unsteady pressure occur on the blade suction side at the vortex-shedding frequency, and these affect the integrated load on the airfoil surface substantially. These unsteady pressure variations would result in severe non-synchronous (i.e. not associated with blade rotation) vibration in an operating engine. One regularly encounters non-synchronous vibrations in compressors operating near stall [3, 4], but turbine durability is more usually compromised by unsteadiness due to rotor/stator interaction. Doorly and Oldfield [5] observed instantaneous local separation on a turbine blade in conjunction with shock passing, and their Schlieren images were suggestive of the occurrence of the phenomenon described here in the vicinity of the blade trailing edge.

This report describes the design and numerical analysis of a turbine cascade suitable to research the vortex shedding and shock waves coupling. This follows the very successful research model that was used to drive a 60% increase in lift beyond the state-of-the-art for Low Pressure Turbines (LPTs) in another AFOSR portfolio [6-7]. The selected turbine flow passage enhanced the vortex shedding intensity by using a relatively large trailing edge diameter. This geometry is both government-owned and generic. So, the geometry and all experimental data produced in the study will be distributable throughout the research community, and this can further increase knowledge about the flowfield and additional means to control. A potential solution that is being explored is the use of pulsed cooling ejection to control both the vortex shedding and trailing edge shock patterns, described by Saracoglu et al. [8]. The present research may guide aerodynamic designers to novel concepts to modulate shock waves.

The current research is high relevance for the design of compact and light future fluid machinery. While the results of such an investigation have bearing on transonic turbines and compressors in particular, the physics that dominate the flow are fundamental and could have applicability to any flow that is dominated by both shocks and vortical disturbances.

2. Airfoil design

2.1. Design tool

One hundred rotor blade geometries were designed at AFRL using a complete design and analysis system for turbine airfoils described by Clark et al. [9]. It employs an industry-standard airfoil shape-generation algorithm developed to define turbine blade and vane shapes. The grid generator and flow solver of Ni [10] were used to determine the aero-thermodynamic behavior of the design shapes. The shape and grid generators and the flow solver are then combined with GUI-based flowfield-interrogation and design-optimization techniques to allow a designer to realize new and/or improved airfoils in short order. A combination of optimization tools are available including gradient based (sequential quadratic programming) and genetic algorithms as well as Design of Experiments analysis, and a wide range of objective functions are specifiable by the user (e.g. to reduce loss or to minimize the circumferential distribution in static pressure downstream of the airfoil after Clark [11]).

The imposed inlet total temperatures, total pressures, and flow angles corresponded are listed in the table below. At the outlet, the measured average static pressure P_{s2} was imposed corresponding to a nominal Mach number of 0.95. All the walls were assumed to be adiabatic with no-slip boundary condition.

$T_{0,\ inlet}$	527	r
$P_{0,\ inlet}$	15.32	psi
$P_{s,\ outlet}$	8.402	psi
$\beta_{\ inlet}$	40	deg.

The relative inlet flow angle was 40 deg. with a pitch to chord ratio equals to 1.056. The nominal design Mach number was 0.95.

2.2. First generation of turbine airfoils

A total of a hundred airfoil geometries were first analyzed considering the time-averaged behavior with the solver developed by Ni [10].

The numerical domain reproduced a single flow passage, considering periodic boundary conditions on the upper and lower ends of the domain. The inlet and outlet sections which were inclined according to the stagger angle of the cascade were located 0.5 and 1.5 chords away from the profile leading and trailing edges respectively. The computational mesh was prepared using the tool developed by ADS, WAND. Special attention was paid to the resolution on the wall, the base and the wake regions.

All the simulations were run in a desktop with the following characteristics: AMD Athlon II X2 B24 3 GHz. For the time-averaged simulations 4000 iterations were run resulting in residuals below 10^{-6}. The finest grid (run for airfoil 65) consisted of 111747 elements, which required about 20 hours of computational time to run 4800 iterations.

The analysis of the time-averaged pressure is performed to characterize the flow field aerodynamics in the cascade passage. Based on the steady flow analysis the worst airfoil in terms of losses was number 4. Geometries 2, 5 and 98 had a convergent divergent flow passage. Airfoils 61, 65 and 68 exhibited an over acceleration in the front suction side followed by a sudden increase in pressure. In terms of downstream pressure distortion the airfoil 68 was the best. Fig. 1-left displays the geometry of the most interesting profiles 39 and 68. Both are characterized by a convergent passage within the guided passage by the airfoils. Unfortunately airfoil 68 has a tiny valley of static pressure in the front suction side, which would be very detrimental at off design conditions. Both airfoils exhibit a nearly constant acceleration along the suction side until around x/bx equal to 0.7, where the right running shock of the neighboring airfoil impacts. The deceleration caused by the shock wave is much more intense for airfoil 68 than for the airfoil 39. Then downstream of the shock impact the flow keeps accelerating in both airfoils until the trailing edge.

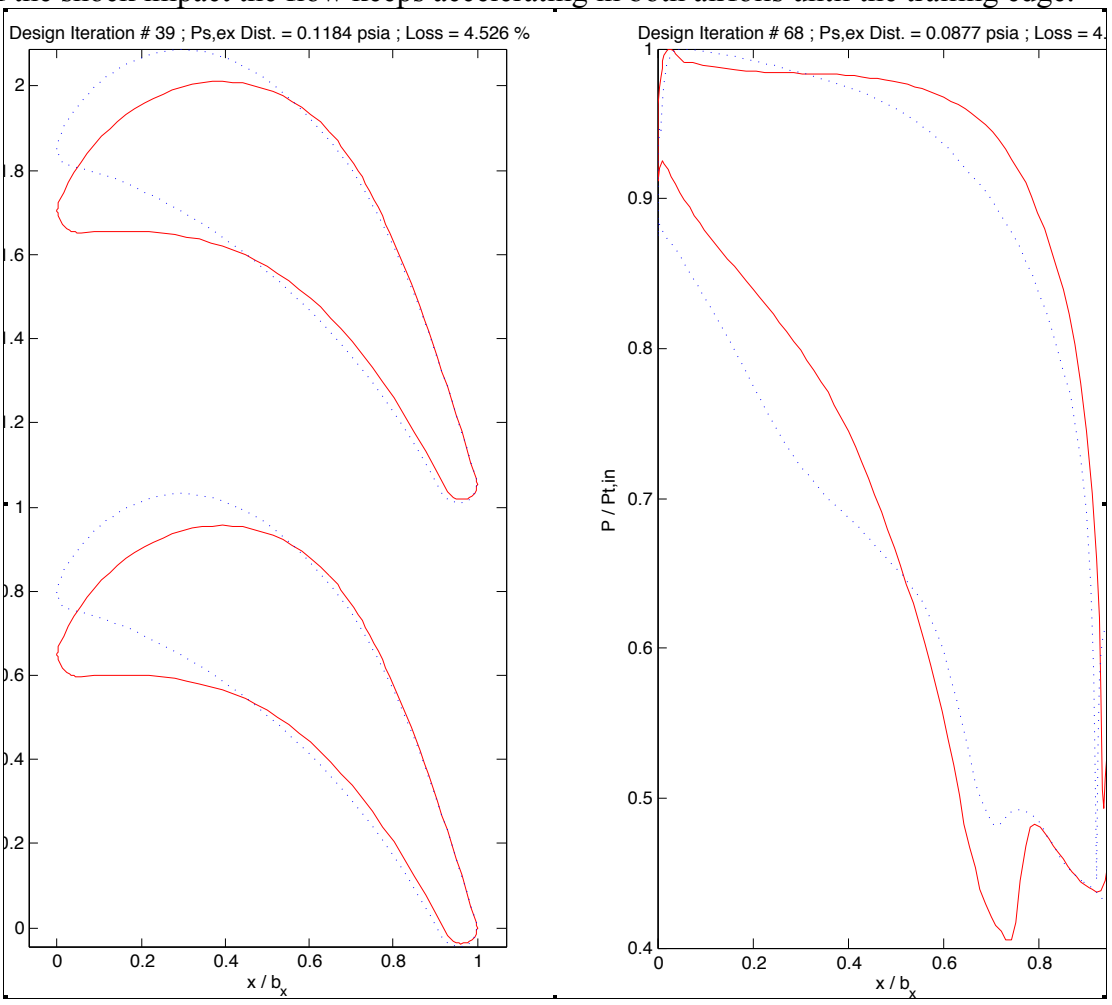

Fig. 1. Left) Geometry of the airfoil 39 (in blue) and airfoil 68 (in red). Right) Static pressure distribution of airfoils 39 (in blue) and airfoil 68 (in red)

2.3. Final redesign of the turbine airfoils

Based on airfoils 39 and 68 several modifications were made to obtain two final airfoils called "39 modified" (obtained by reshaping the leading edge) and "68 plus 20 deg" (increasing the leading edge wedge angle by 20 degrees). Fig. 2 below displays the geometry and the static pressure distribution.

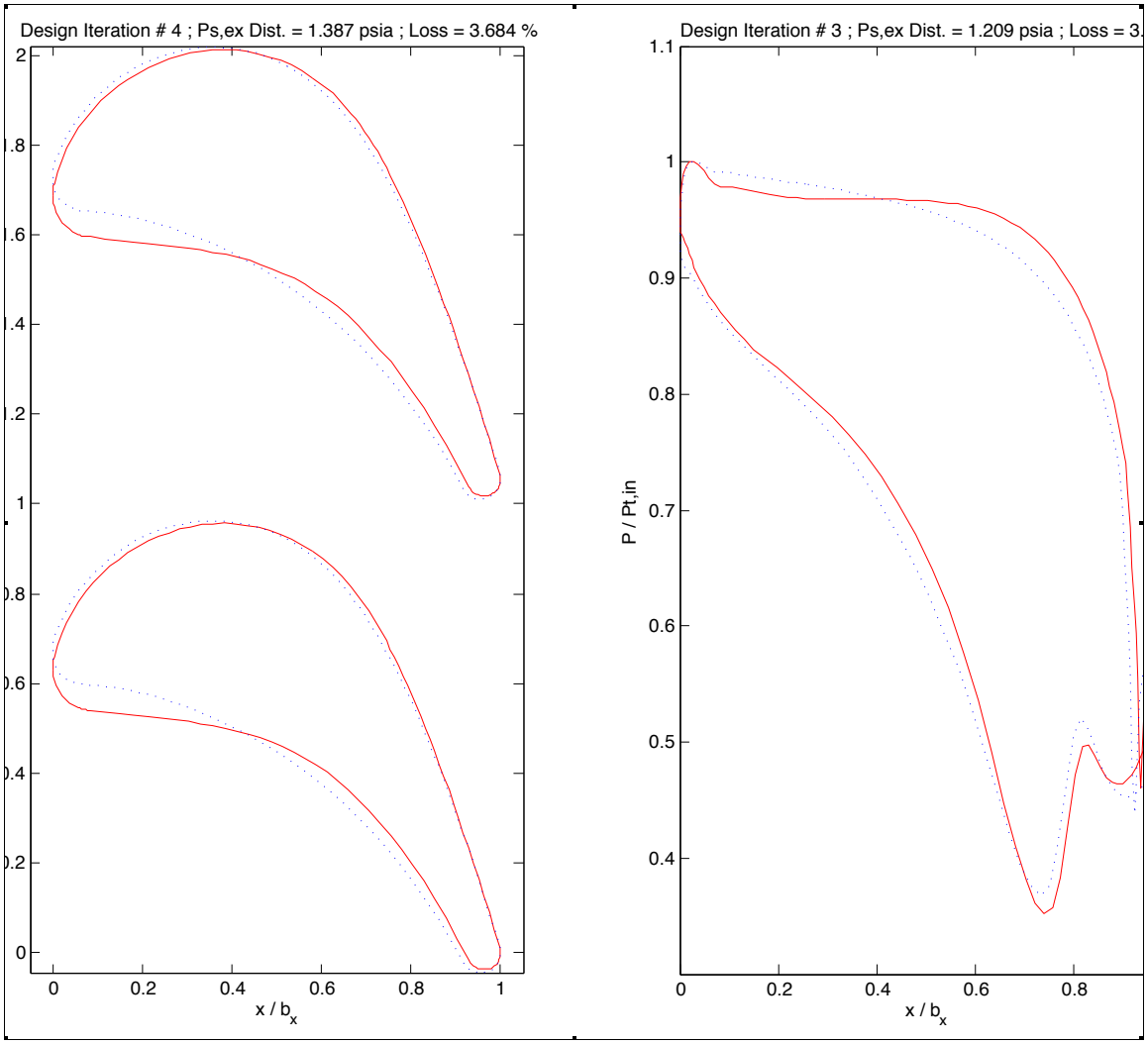

Fig. 2. Left) Geometry of the "airfoil 39" modified (in blue) and "airfoil 68 plus 20" (in red). Right) Static pressure distribution of airfoils 39 (in blue) and airfoil 68 (in red)

Both airfoils exhibit a very similar aerodynamic behaviour. The most striking difference in the loading is the front part of the pressure side. "Airfoil 68 plus 20" experiences a plateau, while the 39 modified has a steady acceleration all along the profile. Additionally, airfoil 39 modified exhibits less difussion in the rear suction side, the lower loading is being compensated in the front pressure side where the airfoil has a smoother rate of acceleration. Hence, the modified 39 airfoil is the selected geometry.

3. Off-design analysis of the modified 39 airfoil

Fig. 3 represents the isentropic Mach number distribution for several outlet Mach numbers ranging from 0.6 to 1.1 for the modified 39 and 68 airfoils. Both experience a very similar behavior. In the subsonic range, the modified 39 has a lower rate of diffusion in the rear suction side, while in the supersonic range 39 has a more abrupt difussion. For a supersonic outlet Mach number 1.05 one can observe that the pressure decrease caused by the shock impact is larger in the airfoil 39, and likewise the extent of the acceleration caused by the expansion fan is larger. Hence one would expect a stronger shock in the case of airfoild 39.

$$M_{is} = \sqrt{\left(2/(\gamma-1)\right)\left(\left(P_{01}/P_s\right)^{(\gamma-1)/\gamma} - 1\right)}$$

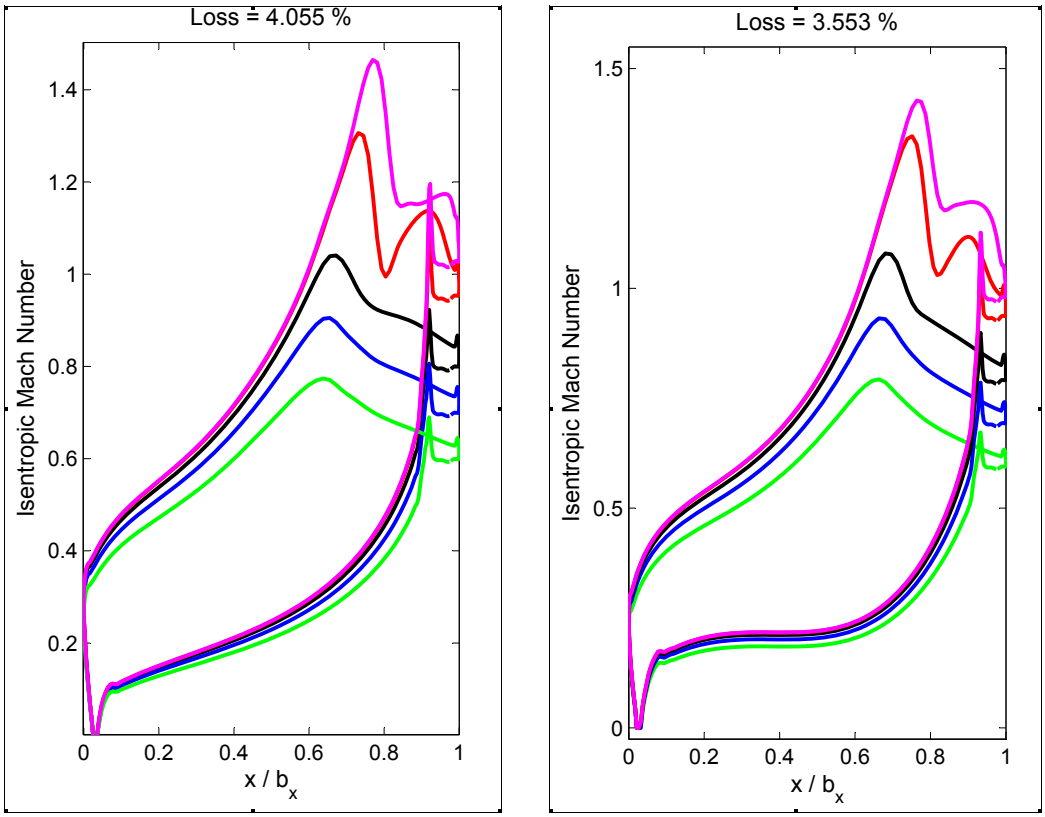

Fig. 3. Isentropic Mach number distributions for several outlet static pressure for the "airfoil 39 modified" (on the left) and "airfoil 68 plus 20" (on the right)

Fig. 4 displays the static pressure envelope resulting from the URANS calculations. Interestingly in a ducted flow with a lower rate of difussion, in the airfoil 39 modified the instabilities from the vortex shedding are transmitted upstream with higher effect than from the 68.

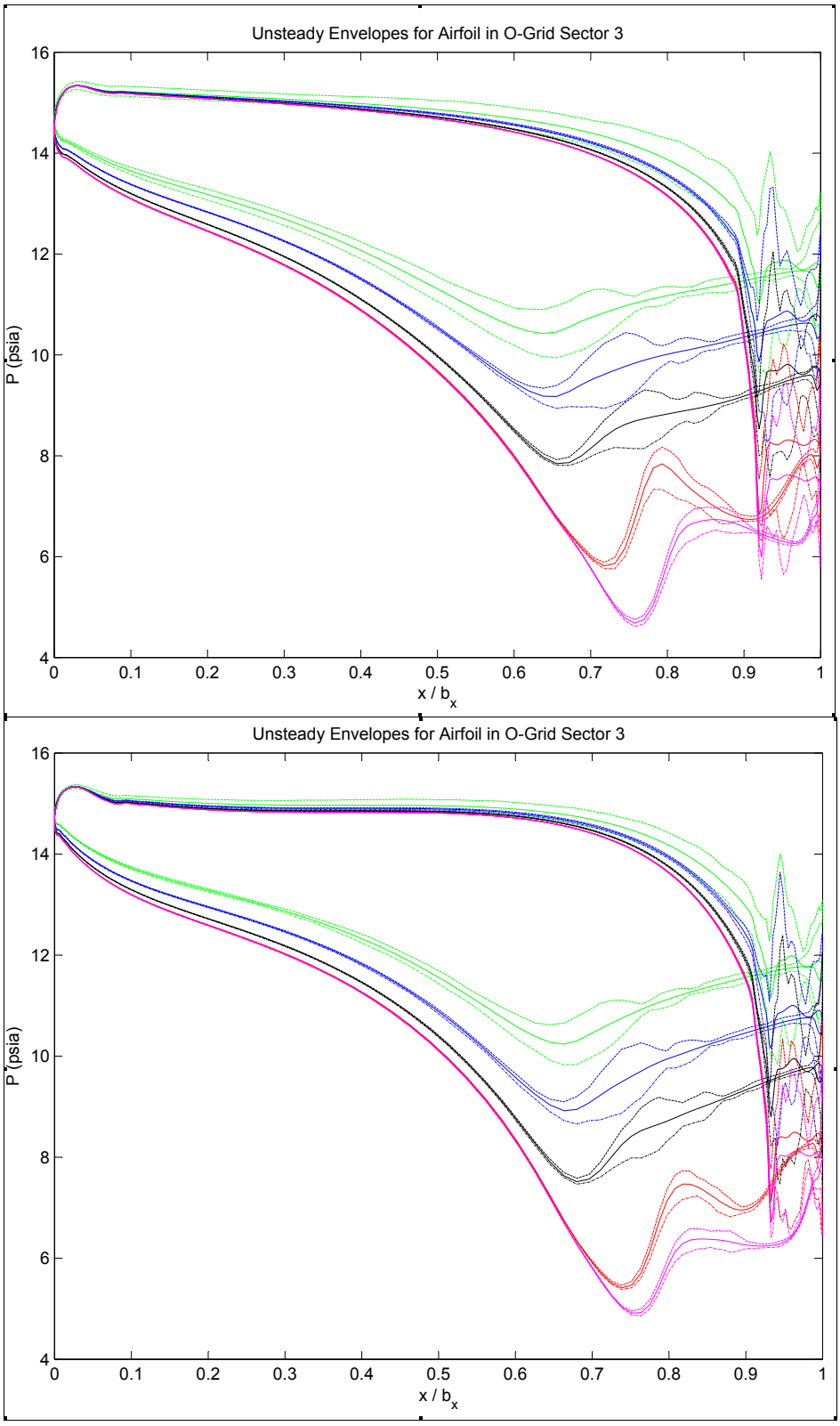

Fig. 4. Unsteady static pressure envelope for several outlet Mach numbers for airfoil 39 modified (top) and for the 68 plus 20 (bottom)

4. Final airfoil geometry

The selected transonic turbine airfoil is the modified 39, whose geometrical coordinates in (x,y) is listed below:

X	Y
1.947890	-0.081632
1.939370	-0.085072
1.930540	-0.087623
1.921500	-0.089261
1.912330	-0.089968
1.903140	-0.089737
1.894020	-0.088568
1.885070	-0.086477
1.876380	-0.083481
1.868030	-0.079613
1.860130	-0.074914
1.852760	-0.069415
1.845990	-0.063191
1.839840	-0.056342
1.834480	-0.048932
1.829600	-0.041132
1.824490	-0.032072
1.818720	-0.022123
1.812570	-0.011143
1.806060	0.000839
1.799160	0.013770
1.791850	0.027621
1.784130	0.042350
1.775840	0.057850
1.766710	0.073933
1.756880	0.090646
1.746540	0.108060
1.735640	0.126115
1.724180	0.144778
1.712150	0.164013
1.699550	0.183786
1.686380	0.204062
1.672630	0.224805
1.658310	0.245980
1.643420	0.267549
1.627940	0.289477
1.611890	0.311728
1.595260	0.334264
1.578060	0.357049
1.560280	0.380046
1.541920	0.403219
1.523000	0.426529
1.503510	0.449942

1.483450	0.473419
1.462850	0.496925
1.441690	0.520425
1.420000	0.543881
1.397780	0.567259
1.375050	0.590525
1.351810	0.613643
1.328080	0.636582
1.303870	0.659309
1.279200	0.681791
1.254100	0.703998
1.228570	0.725901
1.202650	0.747471
1.176340	0.768681
1.149680	0.789505
1.122700	0.809918
1.095410	0.829897
1.067840	0.849420
1.040030	0.868467
1.012000	0.887020
0.983784	0.905061
0.955414	0.922575
0.926923	0.939548
0.898343	0.955969
0.869710	0.971827
0.841058	0.987113
0.812423	1.001820
0.783840	1.015940
0.755347	1.029480
0.726979	1.042420
0.698775	1.054780
0.670771	1.066540
0.643005	1.077720
0.615513	1.088310
0.588335	1.098320
0.561507	1.107760
0.535066	1.116640
0.509050	1.124950
0.483496	1.132730
0.458440	1.139960
0.433919	1.146670
0.409970	1.152860
0.386628	1.158560
0.363929	1.163780
0.341907	1.168520
0.320599	1.172810
0.300038	1.176660
0.280258	1.180090
0.261295	1.183110

0.243180	1.185750
0.225947	1.188010
0.209628	1.189930
0.194257	1.191510
0.179862	1.192760
0.166476	1.193690
0.154134	1.194340
0.141801	1.195140
0.129508	1.196410
0.117308	1.198380
0.105256	1.201130
0.093419	1.204680
0.081875	1.209100
0.070719	1.214420
0.060068	1.220690
0.050044	1.227920
0.040735	1.236060
0.032272	1.245070
0.024777	1.254890
0.018308	1.265430
0.012810	1.276510
0.008290	1.288010
0.004797	1.299860
0.002320	1.311970
0.000758	1.324230
0.000044	1.336570
0.000108	1.348930
0.000888	1.361270
0.002325	1.373540
0.004362	1.385730
0.006952	1.397820
0.010048	1.409780
0.013613	1.421620
0.017610	1.433310
0.022009	1.444860
0.026757	1.456270
0.032591	1.469440
0.039572	1.484280
0.047768	1.500700
0.057225	1.518590
0.068044	1.537840
0.080341	1.558310
0.094212	1.579840
0.109753	1.602300
0.127057	1.625500
0.146211	1.649280
0.167293	1.673450
0.190375	1.697820
0.215515	1.722160

0.242761	1.746270
0.272144	1.769920
0.303681	1.792860
0.337373	1.814850
0.373199	1.835630
0.411116	1.854930
0.451059	1.872480
0.492936	1.887990
0.536624	1.901180
0.581967	1.911770
0.628777	1.919480
0.676827	1.924050
0.725854	1.925240
0.775562	1.922850
0.825628	1.916710
0.875706	1.906730
0.925442	1.892860
0.974490	1.875130
1.022520	1.853620
1.069230	1.828490
1.114380	1.799940
1.157740	1.768220
1.199180	1.733590
1.238560	1.696330
1.275840	1.656740
1.311000	1.615110
1.344310	1.571900
1.376070	1.527530
1.406390	1.482200
1.435370	1.436110
1.463120	1.389430
1.489730	1.342320
1.515270	1.294890
1.539830	1.247260
1.563450	1.199560
1.586200	1.151870
1.608140	1.104290
1.629300	1.056890
1.649720	1.009780
1.669440	0.963008
1.688480	0.916661
1.706880	0.870807
1.724660	0.825511
1.741830	0.780841
1.758410	0.736858
1.774420	0.693625
1.789870	0.651202
1.804770	0.609648
1.819130	0.569020

1.832960	0.529377
1.846250	0.490775
1.859010	0.453268
1.871250	0.416912
1.882970	0.381762
1.894160	0.347871
1.904830	0.315292
1.914970	0.284078
1.924570	0.254283
1.933650	0.225958
1.942180	0.199154
1.950160	0.173925
1.957590	0.150320
1.964440	0.128386
1.970790	0.108197
1.976710	0.089834
1.982180	0.073346
1.986930	0.058691
1.990800	0.045880
1.993830	0.034984
1.996230	0.026112
1.998260	0.017153
1.999540	0.008055
1.999980	-0.001118
1.999320	-0.010285
1.997880	-0.019361
1.995460	-0.028224
1.992140	-0.036790
1.987960	-0.044974
1.982960	-0.052690
1.977210	-0.059855
1.970760	-0.066397
1.963670	-0.072245
1.956020	-0.077342
1.947890	-0.081632

References

[1] Clark, J. P., and Grover, E. A., 2007, “Assessing Convergence in Predictions of Periodic-Unsteady Flowfields,” ASME Journal of Turbomachinery, Vol. 129, pp. 740-749.

[2] Ifeachor, E. C. and Jervis, B. W., 1996, Digital Signal Processing, Addison-Wesley, New York.

[3] Kielb, R. E., Barter, J. W., Thomas, J. P., and Hall, K. C., 2003, “Blade Excitation by Aerodynamic Instabilities – A Compressor Blade Study,” ASME Paper No. GT2003-38634.

[4] Sanders, A. J., 2005, “Non-Synchronous Vibration (NSV) Due to a Flow-Induced Aerodynamic Instability in a Composite Fan Stator,” ASME Journal of Turbomachinery, Vol. 127, pp. 412-421 (Also ASME Paper No. GT2004-53492).

[5] Doorly, D. J. and Oldfield, M. L. G., 1985, “Simulation of the Effects of Shock Wave Passing on a Turbine Rotor Blade,” ASME Journal of Engineering for Gas Turbines and Power, Vol. 107, pp. 998-1006.

[6] Bons, J. P., Pluim, J., Gompertz, K., Bloxham, M., and Clark, J. P., 2012, “The Application of Flow Control to an Aft-Loaded Low Pressure Turbine Cascade with Unsteady Wakes,” ASME Journal of Turbomachinery, Vol. 134, pp. 031009-1-031009-11, (Also ASME Paper No. GT2008-50864).

[7] Lyall, M. E., King, P. I., Sondergaard, R., Clark, J. P., and McQuilling, M. W., 2011, "An Investigation of Reynolds Lapse Rate for Highly Loaded Low Pressure Turbine Airfoils with Forward and Aft Loading," to appear in the ASME Journal of Turbomachinery, (Also ASME Paper No. GT2011-46328).

[8] Saracoglu B.H., Paniagua G, Salvadori S., Tomasoni F., Duni S., Yasa T., Miranda A., 2012, “Trailing edge shock modulation by pulsating coolant ejection”, Applied Thermal Engineering. Vol. 48, pp 1-10. December. DOI: 10.1016/j.applthermaleng.2012.04.036. ISSN: 1359-4311.

[9] Clark, J. P., Koch, P. J., Ooten, M. K., Johnson, J. J., Dagg, J., McQuilling, M. W., Huber, F., and Johnson, P. D., 2009, “Design of Turbine Components to Answer Research Questions in Unsteady Aerodynamics and Heat Transfer,” AFRL Report No. AFRL-RZ-WP-TR-2009-2180.

[10] Ni, R. H., Humber, W., Fan, G., Johnson, P. D., Downs, J., Clark, J. P., and Koch, P. J., 2011, "Conjugate Heat Transfer Analysis of a Film-Cooled Turbine Vane," ASME Paper No. GT2011-45920.

[11] Clark, J. P., 2012, "Design Strategies to Mitigate Unsteady Forcing," in Structural Design of Aircraft Engines: Key Objectives and Techniques, ed. G. Paniagua, NATO Research and Technology Office AVT 207, VKI Lecture Series 2012-06, January.